Spontaneous emission of a two-level atom placed within clusters of metallic nanoparticles

2007 J. Phys.: Condens. Matter 19 096210

(http://iopscience.iop.org/0953-8984/19/9/096210)

IOP PUBLISHING JOURNAL OF PHYSICS: CONDENSED MATTER

J. Phys.: Condens. Matter **19** (2007) 096210 (10pp) doi:10.1088/0953-8984/19/9/096210

Spontaneous emission of a two-level atom placed within clusters of metallic nanoparticles

V Yannopapas[1,2] **and N V Vitanov**[2,3]

[1] Department of Materials Science, University of Patras, GR-26504 Patras, Greece
[2] Department of Physics, Sofia University, James Bourchier 5 boulevard, 1164 Sofia, Bulgaria
[3] Institute of Solid State Physics, Bulgarian Academy of Sciences, Tsarigradsko chaussée 72, 1784 Sofia, Bulgaria

E-mail: vyannop@upatras.gr

Received 24 November 2006, in final form 5 January 2007
Published 14 February 2007
Online at stacks.iop.org/JPhysCM/19/096210

Abstract

We present calculations of the electromagnetic local density of states and of the corresponding spontaneous emission rate for a two-level atom placed near a metallic Drude-type nanosphere as well as within clusters of nanospheres. Our calculations are based on a dyadic Green's function formalism within the framework of the multiple-scattering method. We examine the convergence of the above quantities in terms of the angular expansion of the electromagnetic field. The frequency and spatial dependence of the local density of states and of the corresponding spontaneous emission rate is also studied by depicting the relevant spectra for different cluster sizes and configurations. We have found, in particular, that within the frequency region of the surface–plasmon resonances the spontaneous emission rate is influenced by the near field of the spheres which are closer to the atom, rendering the contribution of the farthest spheres almost negligible. Depending on the distance from the surface of the sphere(s) the spontaneous emission rate in the cluster assumes values which can be several orders of magnitude larger than the corresponding rate in a vacuum. Finally, we examine the differences which arise when an experimentally available dielectric function is employed instead of the Drude type.

(Some figures in this article are in colour only in the electronic version)

1. Introduction

The optical properties of metallic nanoparticles have attracted much interest in recent years due to advances in electron-beam lithography and self-assembly nanofabrication techniques which allow for the preparation of well-defined systems of nanoparticles with a tailored shape, size and arrangement. A variety of new, interesting and potentially useful physical phenomena arise when such systems are excited at the surface plasmon resonance frequencies [1–6]. Although

there have been numerous theoretical studies on assemblies of nanoparticles concerning properties such as absorption/extinction spectra, local field enhancement, nonlinearities, surface enhanced Raman scattering (SERS) spectra, etc, calculations of the local density of states (LDOS) of the electromagnetic (EM) field are still lacking. As has long been known [7], the spontaneous emission (SpE) rate of atoms/molecules/quantum dots can be strongly modified when the rate of quantum fluctuations of the photon field in the surrounding environment differs markedly from that of a vacuum. LDOS is an important quantity, since it essentially provides the SpE rate of atoms/molecules/quantum dots placed within such environments according to Fermi's golden rule [8]. The lack of thorough studies of the SpE rate in the presence of metallic entities is mainly due to the fact that most of the computational methods used for calculating the LDOS in structured reservoirs, e.g. photonic crystals, are based on the plane wave method which can basically treat non-dispersive and non-absorbing constituent materials such as dielectrics with constant permittivity [9–12]. In order to study structures consisting of materials other than dielectrics, one has to resort to on-shell methods such as the transfer matrix method [13] or the multiple-scattering method [14–21]. Up to now, on-shell LDOS calculations have been reported for a single metallic homogeneous [22, 23] or stratified sphere [24, 25].

Within the multiple-scattering framework, one of the possible routes one can follow to calculate the LDOS of the EM field and subsequently the SpE rate is that based on the dyadic Green's function formalism. Such an approach has been developed for two-dimensional (2D) [26] and three-dimensional (3D) systems of cylindrical [27, 28] and spherical scatterers [29]. The latter work on spherical scatterers is based on a more general treatment of the dyadic Green's function of a wavevector field [30]. Namely, the LDOS is provided by the imaginary part of the trace of the dyadic Green's function of the system which can either be a cluster of a finite number of scatterers or an infinite periodic array of scatterers. Since multiple-scattering theory treats the single-sphere scattering in terms of Mie theory [31], the scatterers can be made of dispersing and/or absorbing materials such as metals or polar crystals.

In this paper, we first provide a brief summary of the multiple-scattering dyadic Green's function formalism. Based on this, we calculate the LDOS and the corresponding SpE rate from a single metallic Drude-type sphere. We examine the speed of convergence of the LDOS in terms of the angular momentum expansion of the EM field. LDOS is depicted as a function of frequency (spectrum) for different distances from the centre of the sphere as well as a function of distance for a specific frequency (dipole plasmon frequency). Then we proceed to calculations of the SpE rate for a single sphere and for clusters of Drude spheres of various arrangements such as linear chains, square or hexagonal clusters, etc. We find in particular that the LDOS spectrum of a given point in space is principally determined by the spheres residing in the immediate vicinity of this point and less by farther spheres. We also find that, around the surface plasmon frequencies, the actual arrangement of the spheres is not important for the SpE rate as long as the spheres are placed at equal distances from the point for which the LDOS is calculated. Finally, in order to bring theory closer to experiment, we repeat some of the SpE rate calculations considering a specific type of sphere, namely gold spheres, by employing an experimentally available dielectric function for gold instead of the Drude formula.

2. Theory

We consider a collection of N_s non-overlapping spherical scatterers described by a permittivity ϵ_s and permeability μ_s centred at sites $\mathbf{R}_n$ in a homogeneous host medium described by ϵ_h, μ_h, respectively. Using site-centred position vectors, the dyadic Green's function for the system of

spheres satisfies [29, 30]

$$\sum_i \left[\omega^2 \delta_{i''i} - \Lambda_{i''i}(\mathbf{R}_n + \mathbf{r}_n)\right] G_{ii'}(\mathbf{R}_n + \mathbf{r}_n, \mathbf{R}_{n'} + \mathbf{r}'_{n'}) = \delta_{i''i'}\delta(\mathbf{r}_n - \mathbf{r}'_{n'})\delta_{nn'} \tag{1}$$

where $\mathbf{r}_n = \mathbf{r} - \mathbf{R}_n$, $\mathbf{r}'_{n'} = \mathbf{r}' - \mathbf{R}_{n'}$, and $i, i' = x, y, z$. The operator $\Lambda_{i''i}(\mathbf{r})$ is given by

$$\mathbf{\Lambda}(\mathbf{r}) = \frac{c^2}{\epsilon(\mathbf{r})\mu(\mathbf{r})} \nabla \times \nabla \times \tag{2}$$

and c is the speed of light in a vacuum. It can be verified that the Green's tensor satisfying equation (1) is as follows [30]

$$G_{ii'}(\mathbf{R}_n + \mathbf{r}_n, \mathbf{R}_{n'} + \mathbf{r}'_{n'}) = G^{(s)n}_{ii'}(\mathbf{r}_n, \mathbf{r}'_{n'})\delta_{nn'} - \mathrm{i}\omega \frac{(\epsilon_\mathrm{h}\mu_\mathrm{h})^{3/2}}{c^3} \sum_{LL'} \overline{R}^n_{L;i}(\mathbf{r}_n) D^{n'n}_{L'L} R^{n'}_{L';i'}(\mathbf{r}'_{n'}). \tag{3}$$

The index L denotes collectively the indices Plm, where $l = 1, 2, \ldots$ is the angular momentum number, m the magnetic number ($-l \leqslant m \leqslant l$) and $P = E, H$ denotes the two independent polarization modes. $G^{(s)n}_{ii'}(\mathbf{r}_n, \mathbf{r}'_{n'})$ is the dyadic Green's function for a single scatterer located at $\mathbf{R}_n$ [29]. $D^{nn'}_{LL'}$ are propagator functions and represent the contribution of all possible paths by which a wave outgoing from the n'th sphere produces an incident wave on the nth sphere, after scattering in all possible ways (sequences) by the spheres at all sites including the nth and n'th spheres. They are given by [29, 30]

$$D^{nn'}_{LL'} = \Omega^{nn'}_{LL'} + \sum_{n''} \sum_{L''} D^{nn''}_{LL''} T^{n''}_{L''} \Omega^{n''n'}_{L''L'}. \tag{4}$$

We have found that it is preferable to solve equation (4) iteratively [32] using an appropriate mixing scheme rather than using a linear system solver, as the latter approach diverges in most cases.

The matrix $\Omega^{n''n'}_{L'''L'}$ appearing in equation (4) is called a free-space propagator and transforms an outgoing vector spherical wave about $\mathbf{R}_{n'}$ in a series of incoming vector spherical waves around $\mathbf{R}_n$ [29, 30]. The vector functions $R^n_{L;i}(\mathbf{r}_n)$, $\overline{R}^n_{L;i}(\mathbf{r}_n)$ are the dimensionless eigenfunctions of the operator of equation (2) for a single sphere which are regular at its centre [29, 30]. Finally, the matrix T^n_L is the scattering T-matrix of the spherical scatterer at $\mathbf{R}_n$ and is provided by Mie theory [31].

Given the dyadic Green's function for a collection of scatterers from equation (3), one can readily obtain the LDOS from [29, 30]

$$n(\mathbf{r}, \omega) = -\frac{2\omega}{\pi} \mathrm{Im} \sum_{n=1}^{N_\mathrm{s}} \sum_{i=x,y,z} G_{ii}(\mathbf{R}_n + \mathbf{r}_n, \mathbf{R}_n + \mathbf{r}_n; \omega^2). \tag{5}$$

The LDOS is appropriate for calculating the SpE rate of a randomly oriented dipole source. If the dipole is oriented along a specific direction $\hat{\mathbf{p}}$, the SpE is determined by the projected LDOS (PLDOS)

$$n(\mathbf{r}, \omega; \hat{\mathbf{p}}) = -\frac{2\omega}{\pi} \mathrm{Im} \sum_{n=1}^{N_\mathrm{s}} \sum_{i,i'=x,y,z} p_i G_{ii'}(\mathbf{R}_n + \mathbf{r}_n, \mathbf{R}_n + \mathbf{r}_n; \omega^2) p_{i'}. \tag{6}$$

According to Fermi's golden rule [8], the SpE rate of an atomic dipole with specific orientation is proportional to the PLDOS. If we denote by Γ the SpE rate of an atom decaying inside a structured reservoir (such as the one provided by a finite collection of scatterers) and by Γ_0 the corresponding SpE rate in a homogeneous medium, the relative SpE rate, Γ/Γ_0, is given by

$$\Gamma/\Gamma_0 = n(\mathbf{r}, \omega; \hat{\mathbf{p}})/n_0(\omega) \tag{7}$$

where $n_0 = \sqrt{\epsilon_h \mu_h}\omega^2/3\pi^2 c^3$ is the PLDOS of the homogeneous medium for a certain direction. The LDOS of a homogeneous medium is, of course, three times n_0. We note, however, that the proportionality of the SpE rate with the LDOS is valid only when the atom lies inside a material which exhibits no dispersion [33]. We also note that the presence of absorbing bodies such as metallic particles does not affect the validity of Fermi's golden rule as was shown previously [22, 23]. In this case, the atomic dipole can also decay non-radiatively and the SpE rate given by Fermi's golden rule (equation (7)) is the sum of the radiative and non-radiative decay rates [6, 22, 23, 25]. Having established the formalism in this section, we are able to calculate the desired LDOS and PLDOS functions for single and collections of metal nanoparticles.

3. Results

3.1. Single metallic nanosphere

We begin by considering a single metallic particle which is surrounded by air. An adequate description of the EM response of metals, more specifically of noble metals, is given by the well-known Drude formula [34]

$$\epsilon_s(\omega) = 1 - \frac{\omega_p^2}{\omega(\omega + i\tau^{-1})}, \tag{8}$$

where ω_p is the bulk plasma frequency and τ the relaxation time of the conduction-band electrons of the metal. The radius of the sphere S is taken to be $S = 0.2c/\omega_p$ and the losses $(\tau\omega_p)^{-1} = 0.01$. Since the plasma frequency $\hbar\omega_p$ is of the order of few eV, the corresponding radius of the sphere is of the order of tens of nanometres (see the case of a gold particle below).

Figure 1 shows the PLDOS for various distances r_s from the surface of the above Drude-type nanosphere as calculated by equation (5) where the dyadic Green's function is given by only the first term of equation (3), i.e. $G_{ii'}^{(s)n}(\mathbf{r}_n, \mathbf{r}'_{n'})$ [29]. We have assumed that the test atomic dipole probing the PLDOS is oriented along a radial axis of the sphere. The different curves in each subfigure correspond to different cut-offs, l_{max}, in the angular-momentum (spherical wave) expansion of the EM field. It is obvious that as the atom is placed closer to the surface of the sphere, more terms are needed in the spherical wave expansion in order to ensure the convergence of the PLDOS. For $r_s\omega_p/c = 0.3,\ 0.2$ we obtain satisfactory convergence for $l_{max} = 4$, whilst for $r_s\omega_p/c = 0.1$, $l_{max} = 6$ suffices. However, when we place the atom on top of the surface (but still outside the sphere) it is hard to achieve convergence. From figure 1(d), it is evident that even for $l_{max} = 9$ the convergence is questionable for frequency regions away from resonance structure. We see, therefore, that one has to go beyond the dipole approximation to obtain accurate results for the (P)LDOS, a fact which has also been pinpointed in previous work [6].

The peaks which form the spectral structure of figure 1 stem from the surface plasmon resonances of the nanosphere. The surface plasmon frequencies correspond to poles of the scattering T-matrix of a single Drude sphere, and, in the limit of small sphere radii, they are given by $\widetilde{\omega}_l \simeq \omega_p\sqrt{l/(2l+1)}$, $l = 1, 2, \ldots$ [31]. Using this, one can easily check that the lowest peak in the curves of figure 1 corresponds to the dipole ($l = 1$) surface plasmon, the next peak due to the quadruple ($l = 2$) surface plasmon, and so on. We observe that away from the surface of the sphere the dipole peak is the most prominent one. However, as we place the atom closer to the sphere, the higher-multipole peaks become more evident and, at the surface of the sphere, they are almost 1.5 orders of magnitude larger that the dipole one. This fact also signifies the need for the inclusion of higher than dipole terms for an accurate description of the atom decay near a metallic nanosphere. It is worth noting that the maxima of the corresponding

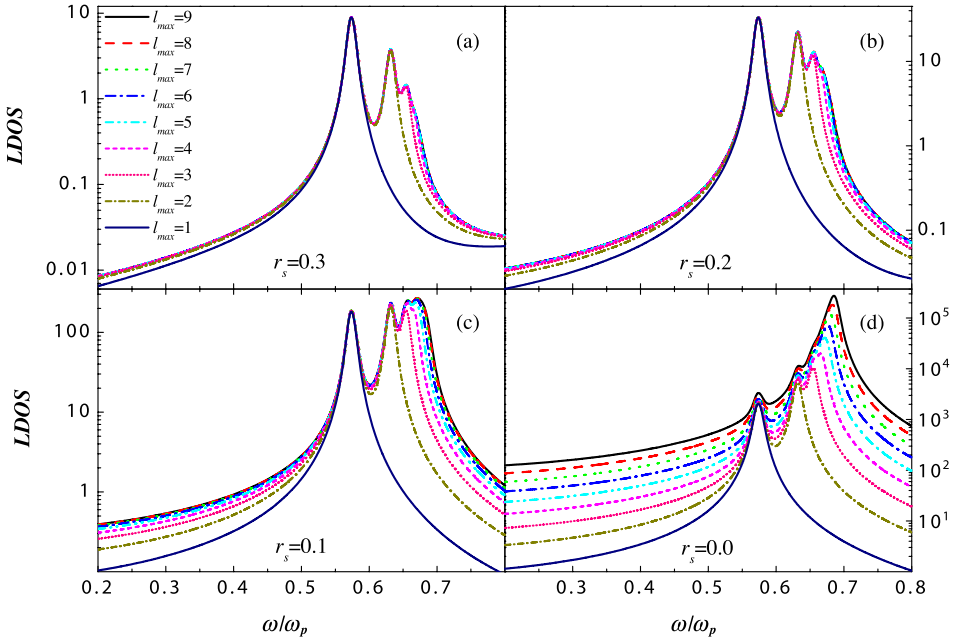

Figure 1. LDOS spectrum for a single Drude [$(\tau\omega_{\rm p})^{-1} = 0.01$] nanosphere ($S\omega_{\rm p}/c = 0.2$) as experienced by an atomic dipole oriented along a radial axis of the sphere for different values of the angular momentum cut-off $l_{\rm max}$ and various distances from the surface of the sphere: (a) $r_{\rm s}\omega_{\rm p}/c = 0.3$, (b) $r_{\rm s}\omega_{\rm p}/c = 0.2$, (c) $r_{\rm s}\omega_{\rm p}/c = 0.1$ and (d) $r_{\rm s}\omega_{\rm p}/c = 0^{+}$.

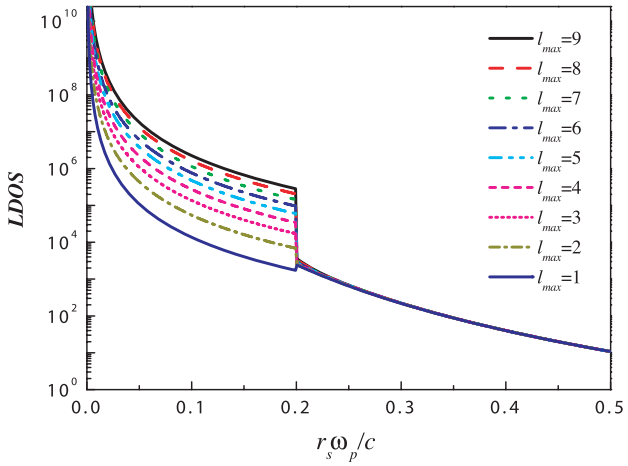

Figure 2. LDOS for a single Drude nanosphere ($S\omega_{\rm p}/c = 0.2$) as a function of the distance from the centre of the sphere, as experienced by an atomic dipole oriented along a radial axis of the sphere, for the first surface plasmon resonance, i.e. for $\omega/\omega_{\rm p} = 1/\sqrt{3}$.

SERS spectra also occur at the surface plasmon frequencies. However, the LDOS spectra are less sensitive to changes in the field strength since LDOS is proportional to the square of the electric field whilst the SERS signal is proportional to the fourth power of the field.

In figure 2 we show the convergence of the PLDOS as a function of the distance from the centre of the sphere for the dipole surface plasmon frequency, i.e. for $\omega/\omega_{\rm p} = 1/\sqrt{3}$. The

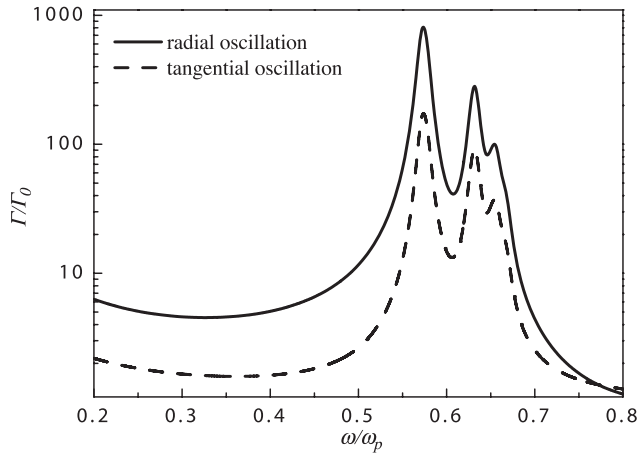

Figure 3. Normalized SpE rate of an atomic dipole which oscillates radially (solid line) and tangentially (broken line) with respect to a Drude sphere of radius $S\omega_p/c = 0.2$ and is placed at a distance $r_s\omega_p/c = 0.5$ from the centre of the sphere. Both curves are calculated for $l_{max} = 4$.

discontinuity of the PLDOS at the surface of the sphere is due to the discontinuous change in the dielectric function. It is obvious that outside the sphere, a small number of spherical waves (small l_{max}) is sufficient for an accurate description of the PLDOS. However, inside the sphere, the convergence is much slower with respect to l_{max} since the description of PLDOS inside the metal sphere is not as accurate as the corresponding one outside the sphere. This is because, within the sphere, the operator of equation (2) is no longer Hermitian due to the complex nature of the dielectric function of the sphere. In this case, the corresponding eigenfunctions do not constitute a complete orthonormal basis and the respective Green's tensor, which is built upon them, is not mathematically correct. PLDOS exhibits a similar behaviour for higher-multipole ($l > 1$) resonance frequencies, except that the discontinuity at the surface of the sphere diminishes gradually as l increases.

Due to the symmetry of the problem, we expect that the PLDOS and the corresponding SpE rate spectra would be different when the atomic dipole oscillates radially or tangentially with respect to the sphere. Indeed, this is what we observe in figure 3: the relative SpE rate Γ/Γ_0 of an atom whose dipole moment is oriented vertically to a radial axis of the sphere is markedly smaller than the corresponding one of a parallel-oriented dipole. The peak value of Γ/Γ_0 for the radially oriented dipole is about 1000 whilst for the tangentially oriented dipole it is about 200. This implies that the coupling with the surface–plasmon states is stronger for a radially oscillating dipole than that for the corresponding tangentially oscillating dipole. This effect will be used for the interpretation of the SpE spectra of an atom placed within a cluster of nanospheres which will follow.

3.2. Cluster of nanospheres

We now examine the influence on the SpE rate of more than one metallic nanosphere. We consider the different arrangements of the spheres shown in figure 4 and calculate the SpE spectra of a two-level atom placed within the cluster. In particular, we are interested in investigating the role of the geometrical arrangement of the spheres on the SpE spectra. Therefore, the distance of the atom from each of the spheres of the cluster is taken to be the

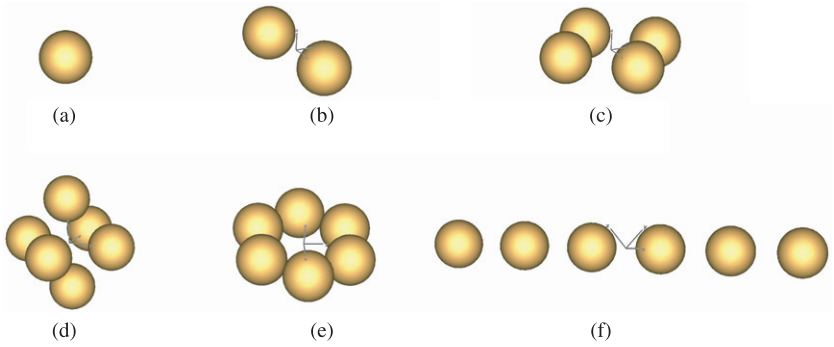

Figure 4. Various clusters of metal nanospheres ($S\omega_p/c = 0.2$) simulated in figures 5–7: (a) single sphere, (b) pair of spheres, (c) square, (d) double-pyramid, (e) hexagon and (f) linear chain. For the clusters (b)–(e) the atom is assumed to be at the centre of symmetry of the structure which is $d = 0.4c/\omega_p$ from the centre of each sphere. At the same distance is placed the atom from a single sphere (a). In the linear chain (f) the sphere centres are a distance c/ω_p apart.

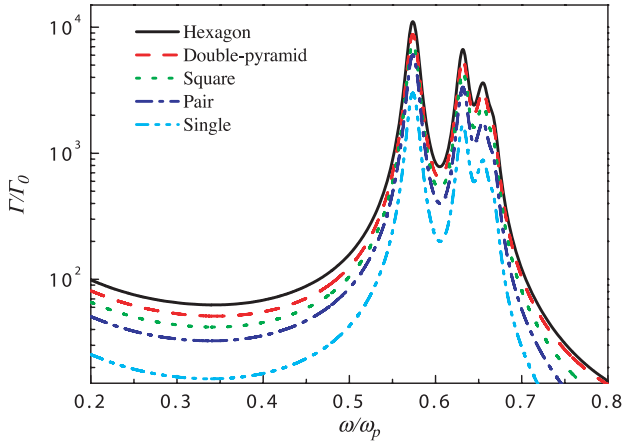

Figure 5. Normalized SpE rate of an atomic dipole oscillating along the x-direction and placed within the clusters (a)–(e) of figure 4: hexagon of Drude spheres (solid (black) line), double pyramid (dashed (red)), square (dotted (green)), pair (dash–dotted (blue)), and near a single sphere (dash–double-dotted (cyan)). In all cases, the distance of the dipole from the centre of the spheres is $d = 0.4c/\omega_p$.

same in the different configurations of figure 4, since the SpE rate decreases very rapidly with distance (see above). The SpE spectra of the different clusters of figure 4 are shown in figure 5. A general trend which is observed in this figure is the progressive increase of the SpE rate with the number of metallic nanoparticles of the cluster which is more obvious in the frequency regions away from the surface–plasmon resonances. This can be easily understood: as we add particles to the cluster, there are more EM states available for the atom to decay to. Of course, this is not generally true; for infinitely periodic dielectric photonic crystals possessing an omnidirectional photonic band gap, as we add more unit cells to a finite cluster of the crystal, the LDOS is suppressed [9–12] in the frequency region of the gap due to interference effects. Another interesting feature of figure 5 is the dependence of the SpE spectrum on the actual arrangement of the spheres, which is evident from the two curves corresponding to clusters

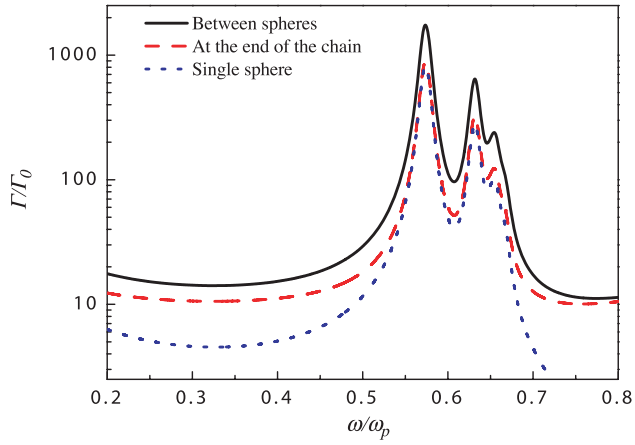

Figure 6. Normalized SpE rate of an atomic dipole which is placed between two Drude nanospheres in the linear chain of figure 4(f) (solid (black) line) at an equal distance $h = 0.5c/\omega_{\rm p}$ from the centre of each sphere and oscillates along the chain axis. The dashed (red) line corresponds to a dipole which is placed outside the chain at the same distance h from the last sphere whilst the dotted (blue) one corresponds to the same distance as well but for a single Drude sphere. All curves are calculated for $l_{\rm max} = 4$.

of six nanoparticles. In particular, the SpE curve for the planar hexagonal cluster (solid line) is overall above the corresponding curve for the 3D double-pyramidal arrangement (dashed line). We attribute this to the dependence of the SpE spectrum on the orientation of the dipole as manifested in figure 3. Since the atom is assumed to oscillate along the x-axis, it is tangentially oriented with respect to the particles which lie on the y- and z-axes. Therefore, the SpE rate for the double-pyramidal arrangement is expected to be lower than that of the hexagonal arrangement, because, in the latter arrangement, the tangential component makes a smaller overall contribution.

Next we consider a linear chain of six equidistant Drude nanospheres. The distance between the spheres is taken to be $a = c/\omega_{\rm p}$. In figure 6 we show Γ/Γ_0 for a two-level atom placed in two different points of the chain: in the middle of the line connecting the third and the fourth sphere (solid line) and at the end of the chain. The choice to put the atom between these two particular spheres is arbitrary, since according to our calculations the solid curve of figure 6 is practically the same for all points in the middle of the line connecting two spheres of the chain. This means that each sphere essentially interacts only with its two neighbouring spheres (first-neighbour interaction) giving rise to a tight-binding description of the EM modes of the chain. The SpE spectrum for an atom placed at the edge of the chain (dashed line) is significantly lower than that within the chain, since for this point the atom essentially experiences the presence of a single sphere. This is evident from the actual coincidence, within the frequency regions of the surface–plasmon resonances, of the dashed curve with the dotted one which corresponds to the SpE rate in the presence of a single Drude nanosphere. As a general comment, the SpE rate within the region of the surface–plasmon resonances is more or less determined by the near-field of the adjacent objects and is practically independent of any farther objects. We have verified that a similar picture (not shown for the sake of brevity) to that of figure 6 is true for an atomic dipole oscillating tangentially to the spheres of the chain except for an overall suppression of the SpE rate, similar to figure 3.

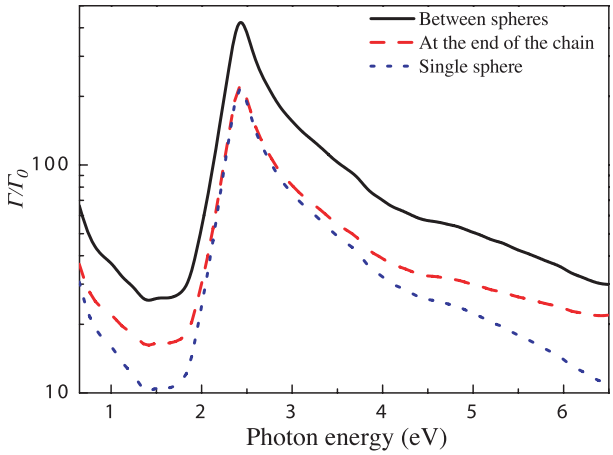

Figure 7. The same as figure 6 only now the metallic spheres are not treated generally as Drude-type spheres but their dielectric function is that of gold and is given by experiment [35].

3.3. Experimental dielectric function

Finally, in order to bring theory closer to experiment, we have employed a more realistic dielectric function for the metallic nanospheres. Namely, we have considered gold nanospheres whose dielectric function is taken from experiment [35]. The advantage is that, apart from the plasmon excitation, it contains all possible sources of absorption such as inter- and intra-band transitions. In figure 7 we show Γ/Γ_0 for the same chain of nanospheres of figure 6 but for the realistic dielectric function of gold [35]. It is evident that for the gold particles, the enhancement of the SpE rate is about three times smaller than that of Drude particles. The SpE rate peak of figure 7 is also present for $l_{\max} = 1$ and, therefore, is of dipolar nature. Other higher-multipole peaks are not apparent, a fact which has also been demonstrated in absorption/extinction spectra from arrays of gold nanospheres [36–38]. In other respects, within the region of the surface–plasmon peak, the SpE spectrum at the end of the chain practically coincides with that of the single gold sphere, similarly to figure 6. We note that the theoretical spectra of figure 7 can be experimentally verified by the use of fluorescence-based techniques [6, 39].

4. Conclusions

Based on a dyadic Green's function multiple-scattering formalism, we have calculated the LDOS and the SpE rate of atoms placed near a metallic nanosphere as well as of atoms within finite clusters of nanospheres. We have shown that in order to have an accurate depiction of the LDOS/SpE rate spectrum one has to consider higher-than-dipole contributions to the EM field. The number of higher-multipole terms needed increases as we move closer to the surface of the sphere(s). When a Drude-type dielectric function is employed for the nanospheres, the higher-multipole terms are also evident as prominent peaks in the LDOS/SpE rate spectra. If a more realistic dielectric function is assumed for the nanospheres, these peaks are absent except from the dipole one. The LDOS and the corresponding SpE rate decrease very rapidly away from the metallic nanospheres and, as a general rule, they are predominantly influenced by the near-field of the nearest neighbours, for frequencies around the region of the surface plasmon resonances. The geometrical arrangement of the nanospheres of the cluster influences the SpE rate (though not dramatically) due to the dependence of the latter on the orientation of the atomic oscillation.

Acknowledgments

This work has been supported by the EU Transfer of Knowledge project CAMEL (grant no. MTKD-CT-2004-014427) and the EU RTN project EMALI (grant no. MRTN-CT-2006-035369).

References

[1] Lamprecht B, Schider G, Lechner R T, Ditlbacher H, Krenn J R, Leitner A and Aussenegg F R 2000 *Phys. Rev. Lett.* **84** 4721
[2] Félidj N, Aubard J, Lévi G, Krenn J R, Schider G, Leitner A and Aussenegg F R 2002 *Phys. Rev.* B **66** 245407
[3] Linden S, Kuhl J and Giessen H 2001 *Phys. Rev. Lett.* **86** 4688
[4] Taleb A, Russier V, Courty A and Pileni M P 1999 *Phys. Rev.* B **59** 13350
[5] Pinna N, Maillard M, Courty A, Russier V and Pileni M P 2002 *Phys. Rev.* B **66** 045415
[6] Anger P, Bharadwaj P and Novotny L 2006 *Phys. Rev. Lett.* **96** 113002
[7] Purcell E M 1946 *Phys. Rev.* **69** 681
[8] Loudon R 1983 *The Quantum Theory of Light* (New York: Oxford)
[9] Li Z-Y, Lin L-L and Zhang Z-Q 2000 *Phys. Rev. Lett.* **84** 4341
[10] Li Z-Y and Xia Y 2001 *Phys. Rev.* A **63** 043817
[11] Wang X-H, Wang R, Gu B-Y and Yang G-Z 2002 *Phys. Rev. Lett.* **88** 093902
[12] Wang X-H, Gu B-Y, Wang R and Xu H-Q 2003 *Phys. Rev. Lett.* **91** 113904
[13] Pendry J B 1994 *J. Mod. Opt.* **41** 209
[14] Ohtaka K 1979 *Phys. Rev.* B **19** 5057
[15] Lamb W, Wood D M and Ashcroft N W 1980 *Phys. Rev.* B **21** 2248
[16] Stefanou N, Karathanos V and Modinos A 1992 *J. Phys.: Condens. Matter* **4** 7389
[17] Stefanou N, Yannopapas V and Modinos A 1998 *Comput. Phys. Commun.* **113** 49
[18] Stefanou N, Yannopapas V and Modinos A 2000 *Comput. Phys. Commun.* **132** 189
[19] Wang X, Zhang X-J, Yu Q and Harmon B N 1993 *Phys. Rev.* B **47** 4161
[20] Moroz A 1995 *Phys. Rev.* B **51** 2068
[21] Moroz A 1999 *Phys. Rev. Lett.* **83** 5274
[22] Ruppin R 1982 *J. Chem. Phys.* **76** 1681
[23] Dung H T, Knöll L and Welsch D K 2000 *Phys. Rev.* A **62** 053804
[24] Moroz A 2005 *Ann. Phys.* **315** 352
[25] Moroz A 2005 *Chem. Phys.* **317** 1
[26] Asatryan A A, Busch K, McPhedran R C, Botten L C, de Sterke C M and Nicorovici N A 2001 *Phys. Rev.* E **63** 046612
[27] Fussell D P, McPhedran R C, de Sterke C M and Asatryan A A 2003 *Phys. Rev.* E **67** R045601
[28] McPhedran R C, Botten L C, McOrist J, Asatryan A A and de Sterke C M 2004 *Phys. Rev.* E **69** 016609
[29] Yannopapas V and Vitanov N V 2007 *Phys. Rev.* B at press
[30] Sainidou R, Stefanou N and Modinos A 2004 *Phys. Rev.* B **69** 064301
[31] Bohren C F and Huffman D R 1983 *Absorption and Scattering of Light by Small Particles* (New York: Wiley)
[32] de Abajo F J G 1999 *Phys. Rev.* B **60** 6086
[33] Nienhuis G and Alkemade C T J 1976 *Physica* C **81** 181
[34] Ashcroft N W and Mermin N D 1976 *Solid State Physics* (New York: Saunders College Publishing)
[35] Johnson R B and Christy R W 1972 *Phys. Rev.* B **6** 4370
[36] Stefanou N and Modinos A 1991 *J. Phys.: Condens. Matter* **3** 8135
[37] Stefanou N and Modinos A 1991 *J. Phys.: Condens. Matter* **3** 8149
[38] Yannopapas V, Modinos A and Stefanou N 2002 *Opt. Quantum Electron.* **34** 227
[39] Lakowicz J R 2001 *Anal. Biochem.* **298** 1